Anal Bioanal Chem (2008) 390:939–946
DOI 10.1007/s00216-007-1723-z

ORIGINAL PAPER

Electrochemical preparation of copper–dendrimer nanocomposites: picomolar detection of Cu^{2+} ions

Sheela Berchmans · T. Mary Vergheese · A. L. Kavitha · Manoj Veerakumar · V. Yegnaraman

Received: 5 September 2007 / Revised: 22 October 2007 / Accepted: 24 October 2007 / Published online: 15 November 2007

Abstract The present work describes, for the first time, in situ electrochemical preparation of dendrimer-encapsulated Cu nanoparticles using a self-assembled monolayer of fourth-generation amine-terminated polyamidoamine (PAMAM) dendrimer as the template. Atomic force microscopy (AFM) and X-ray photoelectron spectroscopy (XPS) studies of the modified surface confirmed the presence of Cu nanoparticles entrapped in dendrimer film. Au electrode modified with a monolayer of the dendrimer enables preconcentration and subsequent voltammetric detection of Cu^{2+} at picomolar concentrations. Further, Cu nanoparticles in the dendrimer monolayer could be electrochemically derivatised to Cu hexacyanoferrate, which exhibits specific crystal planes, unlike the random distribution of crystal planes in bulk-formed Cu hexacyanoferrate, which is another catalytically active material for sensor applications.

Keywords PAMAM dendrimers · Copper–dendrimer nanocomposite · Trace analysis · Copper ions · Templated growth

Introduction

Synthesis of nanostructured materials, possessing very high surface area has made a significant impact in the design of electrochemical platforms for sensors, catalysts, fuel cells, batteries and so on. We report here, for the first time, the electrochemical synthesis, characterization and applications of copper nanocomposites directed by the self-assembly of fourth-generation amine-terminated polyamidoamine (PAMAM) dendrimer ($G4NH_2$). Dendrimers, also known as cascade polymers or arborols, are a new class of materials that have received the attention of research workers at the global level [1–4]. Dendrimers are unique core-shell structures possessing three basic architectural components: a core, an interior of shells (generations) consisting of repeating branching units and terminal groups (the outer shell or periphery). PAMAM dendrimers facilitate the synthesis of metal nanoparticles, since metal ions like Cu^{2+}, Co^{2+}, Pt^{2+} and Pd^{2+} are known to partition into the dendrimer [5–8]. The terminal functional groups like $–NH_2$, –COOH and –OH serve as handles for attaching the dendrimers to electrode surfaces. The interior amine groups complex metal ions, which could be reduced to yield metal nanoparticles encapsulated within the dendrimer cavity. Thus, mono and bimetallic nanoparticles stabilized by dendrimers have been prepared and characterized [9–13]. In all these reports, the metal ions are initially complexed within the dendrimer and then chemically reduced by borohydride ions. Moreover, incorporation of these metal nanoparticles onto electrode substrates without the loss of electrocatalytic activity has been found to be difficult [14, 15]. This work opens up the possibility of growing metal dendrimer nanocomposite in situ on the electrode surface. $G4NH_2$ dendrimer, initially self-assembled on Au surface, serves as a basket for loading catalytically active metal nanoparticles. Copper-modified electrodes have been the subject of interest owing to their electrocatalytic properties. Cu adlayers on Pt electrodes are known to promote the oxidation of formic acid [16]. Microporous deposit of Cu on glassy carbon electrode has been evaluated for the detection of nitrate and nitrite [17, 18]. The preparation of Cu nanoparticles through different approaches has been already reported wherein chemical and

S. Berchmans (✉) · T. M. Vergheese · A. L. Kavitha · M. Veerakumar · V. Yegnaraman
Central Electrochemical Research Institute,
Karaikusi 630006, Taminadu, India
e-mail: sheelaberchmans@yahoo.com

electrochemical preparation have been attempted and the earlier reports are well documented [19]. The utility of Cu nanoparticles have been evaluated for the analysis of substrates like nitrate and nitrite, oxygen, hydrogen peroxide, glucose, *o*-dihydrophenolic compounds etc. The use of dendrimer molecules as surface anchors for the preparation of Cu–dendrimer nanocomposite has been described for the first time in this work.

The metal loading on the electrode surface, modified by dendrimer molecules, can be tuned at will by changing the copper ion concentration in the preconcentration step and this property has been shown to be advantageous for recognition of metal ions at ultra trace levels in biological samples, environmental samples etc. Anodic stripping voltammetry has been routinely used by many researchers for the determination of Cu where the detection limit achieved was of the order of micromolar level only. Analysis of Cu in beer samples has been performed with this method [20]. Amperometric detection of Cu by a yeast biosensor using flow injection analysis has been recently reported wherein the detection limit observed was 16–32 mg L^{-1} [21]. Enhanced detection has been achieved with sonoanalysis and in the presence of surfactants. This kind of enhanced detection has led to submicromolar detection limits [22, 23]. Analysis of Cu in blood has been achieved with the help of sonoelectroanalysis wherein the minimum detection limit achieved is 0.62 ppm of Cu [24]. In this report, we have shown that the multidentate interactions of the dendrimer molecules with the copper ions can lead to a detection limit at the picomolar level.

The interfacially directed growth of Cu–dendrimer nanocomposite within the aqueous shells of dendrimer is demonstrated with the help of atomic force microscopy (AFM) and X-ray photoelectron spectroscopy (XPS) measurements. It has also been shown for the first time that the dendrimer-entrapped metal clusters could be further derivatised to copper hexacyanoferrate whose growth is again dictated by the dendrimer. Compared with randomly oriented crystal growth under bulk conditions, the template-induced crystal growth revealed that only certain growth orientations are preferred. Hexacyanoferrates are one of the longest known coordination compounds, whose redox and electrochromic properties have been extensively studied in basic and technologically oriented research [25–34]. Also the scope for converting the copper nanoparticles into its hexacyanoferrate derivative has been demonstrated for its catalytic and sensing characteristics.

Essentially three objectives have been realized in this paper: (1) the electrochemical preparation of Cu–dendrimer nanocomposite; (2) it is shown that the dendrimer-modified gold substrate can be tuned for preconcentrating Cu ions of different concentrations, which can be sensed by anodic stripping voltammetry: the limit of detection can be extended to picomolar levels by this method; (3) we have explored the structure-directing property of the PAMAM dendriner molecule during the electrochemical derivatisation of Cu–dendrimer nanocomposite into copper hexacyanoferrate films.

Experimental

Apparatus

Cyclic voltammograms were recorded using a Wenking Potentiscan (POS 88) and X-Y/t recorder (Rikadenki) and PARSTAT2263. A conventional three-electrode electrochemical cell was used with a gold electrode as the working electrode, Pt electrode as the counter electrode and an Hg|Hg_2SO_4|H_2SO_4 (0.5 M) (MSE) as reference electrode. For stripping experiments gold disc electrode (φ 2 mm) was used. Gold slides (1,000-Å gold coating on silicon wafers with an intermediate adhesion layer of Ti, 100-Å thickness procured from Lance Goddard associates, USA) of size 1× 1 cm^2 were used for XPS and AFM measurement and for the characterization of copper–dendrimer nanocomposite.

The VG ESCA MK200X was used for XPS analysis. AlK_α X-ray (1,486.6 eV) with 300-W power was used as the exciting source, and a pass energy of 20 eV was used for data collection. The energy analyzer employed was hemispherical with a 150-mm diameter. Vacuum maintained during the experiment was 1.2×10^{-9} mbar.

Atomic force microscopic images were recorded with the Molecular Imaging PicoSPM using gold-coated silicon nitride 30-nm cantilevers (force constant 0.12 N m^{-1}) and CP-II scanning probe microscope (Veeco).

SEM images were taken using an Hitachi S3000-H.

Reagents

All stock solutions were prepared using triply distilled water. PAMAM dendrimer was purchased from Aldrich. Analar grade H_2SO_4 (Merck), $CuSO_4{\cdot}5H_2O$ (Merck), potassium ferrocyanide (Merck) and ruthenium(III) hexamine chloride (Aldrich) were used as received.

In situ electrochemical synthesis of copper–dendrimer nanocomposite (CuDNC)

Gold substrate was immersed overnight in a 0.25 mM solution of fourth-generation PAMAM dendrimer ($G4NH_2$) in ethanol. It was then withdrawn, washed with ethanol, air-dried and then immersed in a 1 mM solution of copper sulfate for 10 min. It is then removed from the solution, washed with water and introduced into an electrochemical cell containing 0.5 M sulfuric acid to electrochemically reduce the Cu^{2+} ions trapped inside the dendrimer monolayer. Pt and Hg/Hg_2SO_4 electrode served as counter and reference electrodes, respectively. The working electrode

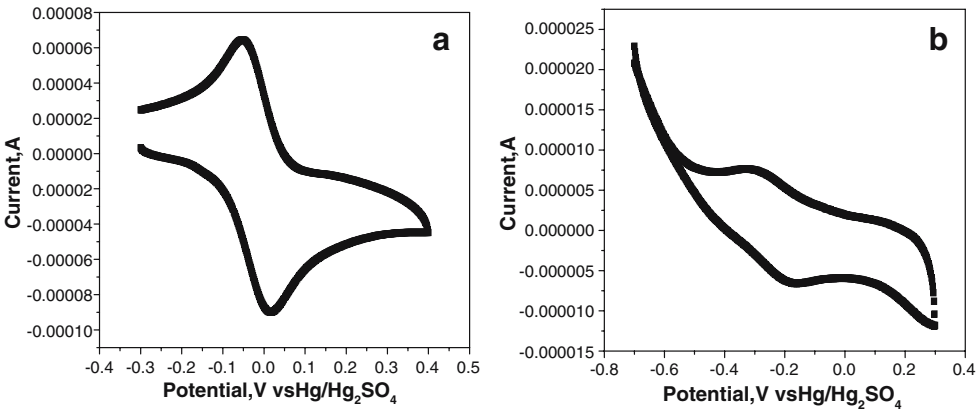

Fig. 1 Cyclic voltammogram representing the response of potassium ferrocyanide on a dendrimer-modified electrode in **a** 0.5 M H_2SO_4 **b** Phosphate buffer pH 7.0. Scan rate 50 mV s^{-1}

was clamped at a potential of −500 mV, i.e. sufficient to reduce the copper ions.

Derivatisation of dendrimer-entrapped Cu nanaoparticles to Cu hexacyanoferrate

The Au | CuDNC electrode was subjected to electrochemical cycling in a solution containing 0.5 mM potassium ferricyanide and 0.5 M each of HCl and KCl for 20 cycles in the potential range from −0.4 to −0.6 V. The electrode was then washed with water and characterized voltammetrically in blank KCl medium.

Results and discussion

Self-assembly of $G4NH_2$ dendrimers on gold surfaces

Gold electrodes, cleaned by standard pretreatment procedures [35], were subjected to the following steps: (i) modification of Au substrate by the self-assembly of $G4NH_2$; (ii) chemical preconcentration of copper ions into the dendrimer cavities; and (iii) electrochemical reduction of the copper ions to yield Cu–dendrimer nanocomposite film. The presence of the dendrimer film on the electrode was ensured by the electron transfer blocking properties of the film compared with the bare electrode. The electron transfer blocking property of the film was investigated by studying the redox behaviour of ferrocyanide anions and ruthenium hexamine cations on the modified electrode. The blocking of electron transfer for the cationic ruthenium hexamine and unblocking for ferrocyanide anions revealed the presence of dendrimers on the surface.

Figure 1a shows that a reversible electron transfer response was observed for the negatively charged $[Fe(CN)_6]^{4-/3-}$ in acidic medium on the modified electrode. Figure 1b shows the electron transfer characteristics for the negatively charged Fe $(CN)_6]^{4-}$ ions in phosphate buffer medium. The current is very much lowered in phosphate buffer medium and the reversibility is also affected to some extent. The tertiary amine group and the end primary amine group of the PAMAM dendrimer have pK_a values of 5.5 and 9.6, respectively. As pH increases, the deprotonation of tertiary amine groups takes place after pH 5.5 and the interaction of the film with negatively charged ferrocyanide ions decreases. Thus, $[Fe\ (CN)_6]^{4-/3-}$ electron transfer is not completely blocked over a wide range of pH on a dendrimer-modified electrode.

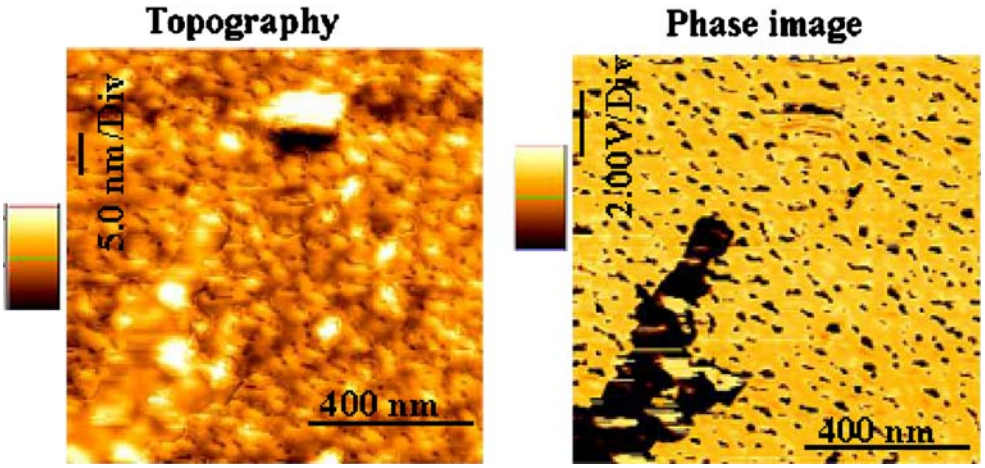

Fig. 2 AFM image of gold substrate modified by the self-assembly of fourth-generation amine-terminated dendrimer

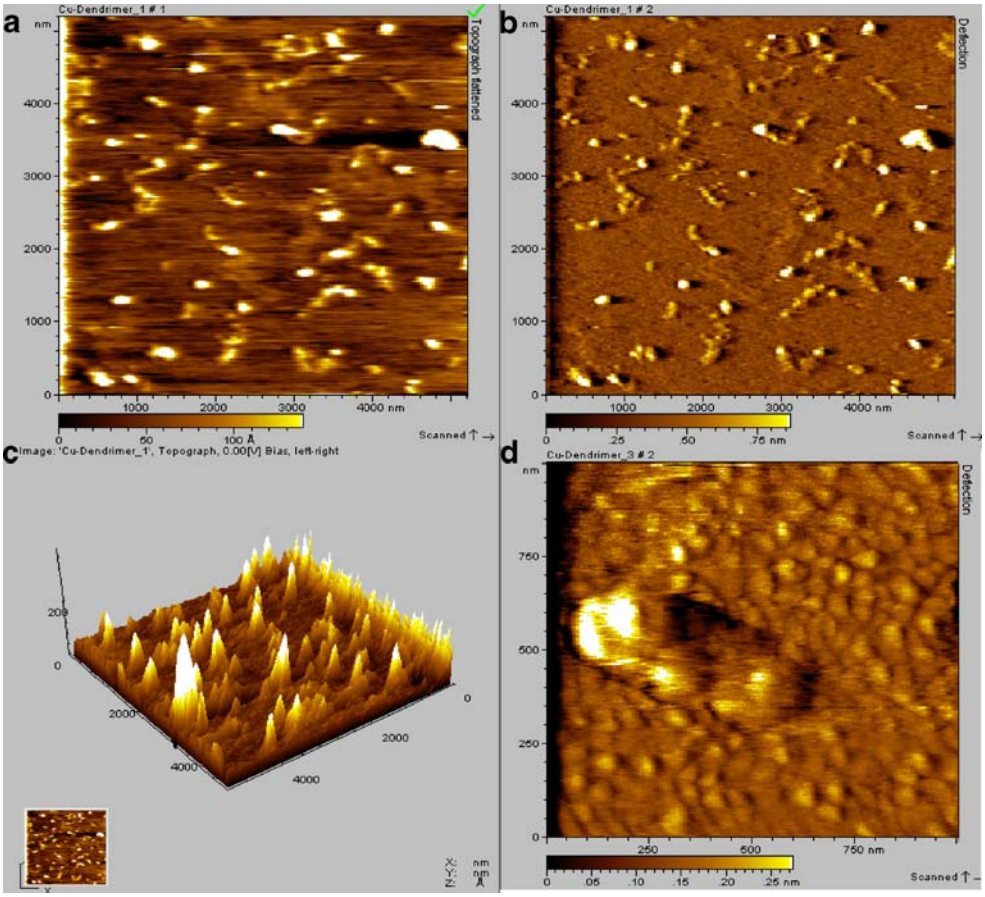

Fig. 3 AFM images: **a** two-dimensional topographic view, **b** deflection image of Au | CuDNC, **c** three-dimensional view and **d** enlarged image of a single CuDNC particle

Similar voltammetric experiments with $[Ru(NH_3)_6]^{2+/3+}$ in acidic and neutral media revealed the absence of redox behaviour on modified electrode (data not shown). It is expected that in both media the dendrimer remains positively charged. Below pH 5.5, the tertiary and primary amine groups remain protonated; beyond pH 5.5, primary amines remain protonated. The positively charged dendrimer molecules are electrostatically attracted by the negatively charged ferrocyanide anions and the electron transfer is therefore not blocked. In the case of positively charged $[Ru(NH_3)_6]^{3+}$ ions, the positively charged dendrimer molecules exert repulsive electrostatic interactions and hence the electron transfer is blocked completely.

The formation of dendrimer film on Au surface through self-assembly is also confirmed by AFM measurements.

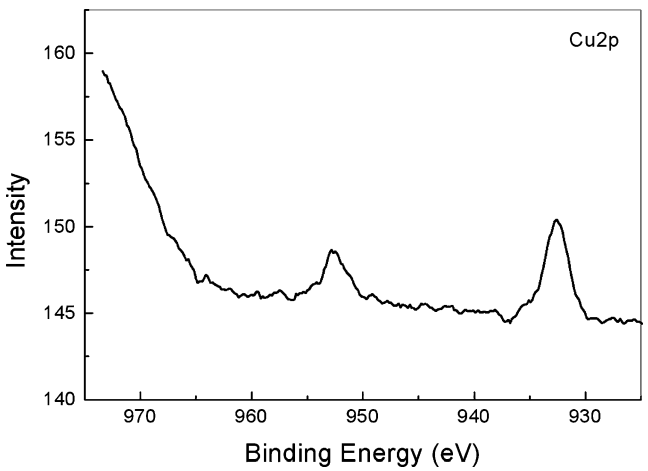

Fig. 4 XPS of Cu–dendrimer nanocomposite electrode

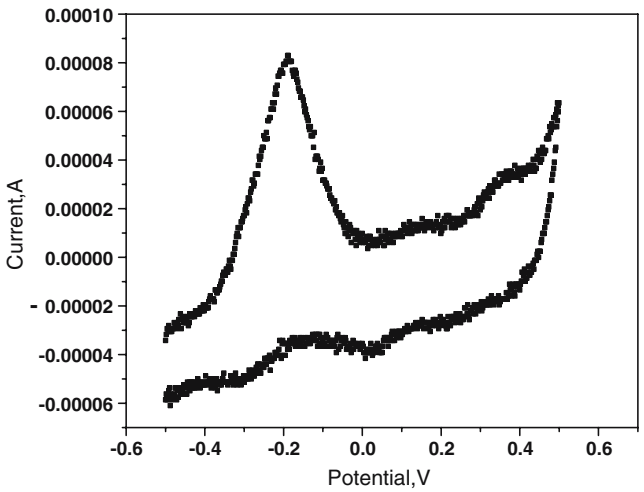

Fig. 5 Cyclic voltammogram representing the response of Cu–dendrimer nanocomposite electrode in 0.5 M sulfuric acid. Scan rate 50 mV s^{-1}

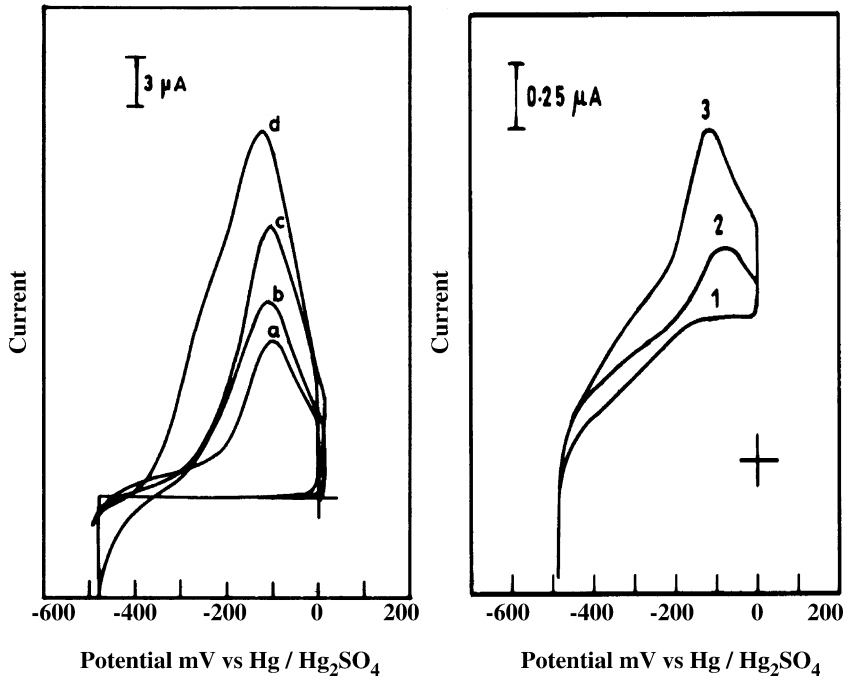

Fig. 6 Anodic stripping voltammograms for different concentrations of Cu(II) in acetate buffer. The concentration of Cu (II) ions used for preconcentration is *a* 1×10^{-3} M, *b* 2×10^{-3} M, *c* 3×10^{-3} M, *d* 5×10^{-3} M; *1* 2×10^{-11} M, *2* 5×10^{-10} M, *3* 2×10^{-9} M

The AFM image of the dendrimer-modified gold substrate is given in Fig. 2. The dendrimer molecules are assembled regularly on the gold substrate. The average height of the assembled layer is nearly 5.0±0.5 nm, which indicates a monolayer of dendrimer self-assembled on Au substrate [36]. From this we presume that the dendrimer molecules align themselves in a vertical orientation as explained in the case of self-assembly of phenanthroline–Au(111) bonding where the authors have observed that phenanthroline molecules interact with the Au(111) surface through nitrogen atoms and are aligned in a vertical fashion, whereas on HOPG the molecules are found to lie flat [37]. The dendrimer-modified Au surface provides an ideal platform for preconcentration of metal ions.

Characterisation of copper–dendrimer nanocomposite

Figure 3 presents the AFM image of Cu–dendrimer nanocomposite obtained after electrochemical reduction of the dendrimer film chemically preconcentrated with copper ions. The particles, in the size range of 75–125 nm, are distributed randomly on the surface. Some of the particles are aggregated and exhibit a size of around 200 nm (Fig. 3d). The dendrimer cavities trap the copper ions, which are electrochemically reduced and entrapped inside the dendrimer through strong complexation by the interior functional groups. Thus this novel methodology enables the dendrimer to be loaded with copper ions that are then electrochemically reduced to yield dendrimer-encapsulated Cu nanoparticles; the dendrimer thus acts as a template, controls particle size and prevents agglomeration. Figure 3c shows that the particles oriented in certain directions.

Figure 4 depicts the XPS response of the Cu–dendrimer nanocomposite film obtained from a 5 mM Cu^{2+} solution. The peaks corresponding to $Cu2p_{3/2}$ and $Cu2p_{1/2}$ appear at 932.7 eV and 932.5 eV, respectively [38]. These results confirm that the copper ions inside the dendrimer film undergo reduction and are present as Cu atoms trapped

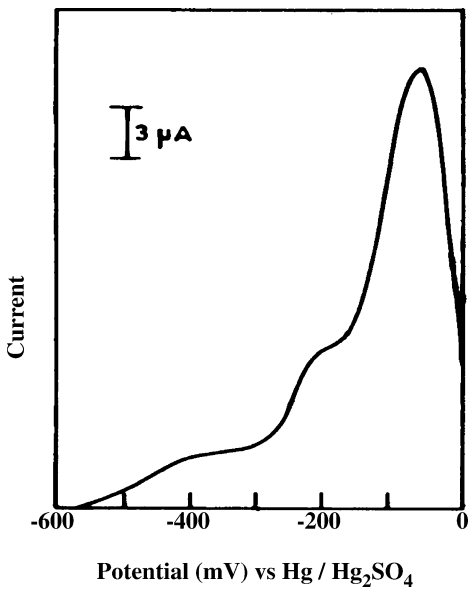

Fig. 7 Anodic stripping voltammogram for 1×10^{-3} M Cu^{2+} in the presence of 1×10^{-4} M each of Bi^{3+} and Cd^{2+} ions in 1 mM acetate buffer (pH 4.5). Scan rate 50 mV s^{-1}

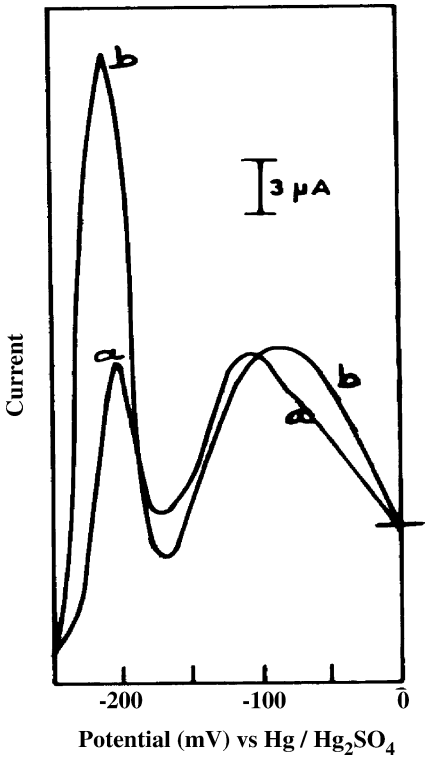

Fig. 8 Anodic stripping voltammogram for 1×10^{-3} M Cu^{2+} in the presence of *a* 1×10^{-3} M Bi^{3+} and *b* 2×10^{-3} M Bi^{3+}

inside the film. This approach opens up a novel methodology for in situ preparation of metal–dendrimer nanocomposites directly on the electrode surface by an electrochemical route.

Figure 5 shows the voltammetric response of Cu–dendrimer nanocomposite formed on Au substrate in 0.5 M sulfuric acid. The anodic peaks appear at −0.18 V, 0.16 V and 0.35 V. Two cathodic peaks appear at 0.02 V and −0.32 V. The anodic peak appearing at −0.18 V corresponds to the bulk-deposited Cu, and the other two anodic peaks correspond to underpotential deposition (upd) of copper. The two peaks corresponding to Cu upd may arise due to Cu adlayers arising from two different ordered phases. The cathodic peak at 0.021 V corresponds to Cu upd and the one occurring at −0.021 V corresponds to bulk Cu. The phenomenon of upd indicates the onset of deposition of metal adatoms at various types of substrates in potential ranges positive to the reversible Nernst potential. The occurrence of upd is, in general, inferred from cyclic voltammetric studies wherein peaks corresponding to sub-monolayer adsorption are observed at potentials more positive than Nernst potential. Thus the charge involved in the adsorption and deposition process can be conveniently analysed by integrating the observed current response over the entire time domain. Because the origin of this phenomenon lies in the enhanced interaction of depositing metals with foreign substrates, the work function differences play a predominant role in dictating the potential shift. The Cu concentration in the monolayer, estimated by charge integration of the anodic peaks, is 550 μC cm^{-2} for bulk deposition and for upd it corresponds to 20 μC cm^{-2}. The charge associated with the two upd peaks were taken into account for the calculation. The charge associated with the Cu upd phenomenon is very small and this implies that the amount of free gold surface available for upd is low. In other words the coverage of dendrimer on the gold surface is nearly maximum and hence only very little space is available as bare gold for upd to occur. The charge corresponding to the bulk Cu deposit is slightly greater than that expected for a monolayer coverage [39]. The Cu concentration inside the film can be controlled by varying the copper ion concentration in solution and the preconcentration time. This implies that the loading of Cu ions inside the dendrimer can be tuned at will. By fixing the preconcentration time and by varying the metal ion concentration, we can use the metal encapsulation property of the dendrimer for trace analysis of Cu ions. This shows the effect of numerous complexing sites available within the dendrimer. The structural architecture of the dendrimer offers an ideal environment to trap guest species. The dendrimer monolayer on the modified substrate can act as an array of molecular baskets, allowing relatively higher loading of metal atoms.

Recognition of copper ions at trace levels

The fact that Cu concentration inside the film can be controlled by varying the copper ion concentration in

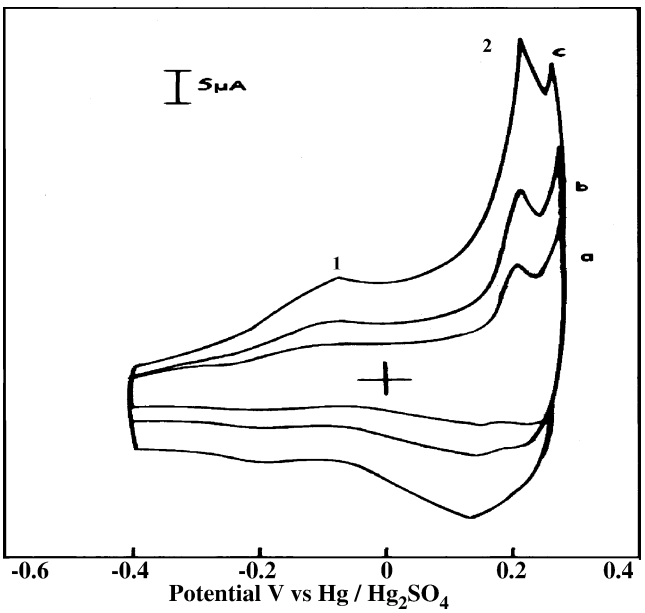

Fig. 9 Represents cyclic voltammograms corresponding to a PAMAM dendrimer self-assembled on gold surface derivatised as copper hexacyanoferrate. Scan rate (mV s^{-1}) *a* 50, *b* 100, *c* 200. Peaks corresponding to CuHCF (*2*) and unreacted copper (*1*) are marked

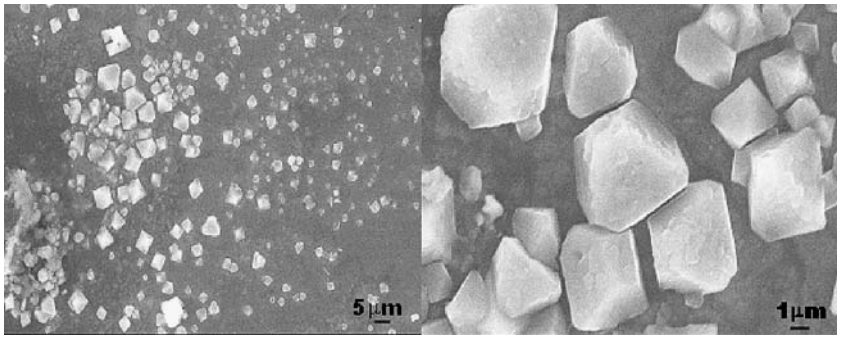

Fig. 10 SEM image of CuHCF film formed by electrochemical derivatisation of Cu–dendrimer nanocomposite electrode

solution offers an analytical methodology for estimating copper ions present at ultra trace levels. To study the interference of other ions like Cd^{2+} and Bi^{3+} the analysis conditions were optimized at pH 4.5 using acetate buffer. In acetate buffer the peak corresponding to bulk-deposited Cu shifts to −0.1 V and this peak is considered for the analysis of Cu. Figure 6 depicts the stripping voltammograms for different concentrations of cupric ions. The voltammograms were recorded in acetate buffer (pH 4.5). It can be seen that the stripping current increases proportionally with the concentration of copper ions in solution and concentrations down to 10^{-12} M levels gives rise to measurable current signals. This implies that the detection limit can be pushed down further by resorting to differential pulse anodic stripping voltammetry. The linear fit between the peak current concentrations yields a correlation coefficient of 0.99784 and the equation of the fitted straight line is $I=0.2948+3.69\ C$. The interference of ions like Cd^{2+} and Bi^{3+} on the recognition was studied and the recognition of copper was not affected by their presence. This experiment demonstrates that the amount of copper ion loading inside the dendrimer can be tuned to will by changing the cupric ion concentration in the preconcentration solution and the stripping currents are proportional to the copper loading inside the dendrimer.

Effect of interferent ions

The anodic stripping voltammetric response for 1×10^{-4} M each of Bi^{3+} and Cd^{2+} ions in the presence of 1 mM Cu^{2+} in acetate buffer of pH 4.5 is presented in Fig. 7. The stripping peak at −400 mV corresponds to Cd^{2+}; the peak at −200 mV corresponds to Bi^{3+}; and the peak at −100 mV corresponds to Cu^{2+}. The three metal ions are well resolved along the potential axis. Figure 8 shows the effect of preconcentration of two different concentrations of Bi^{3+} (1 mM and 2 mM) solutions in the presence of 1 mM Cu^{2+} solution. As the concentration of Bi^{3+} increases, the second cathodic peak at −200 mV increases indicating that the peak appearing at −200 mV corresponds to that of Bi.

Electrochemical derivatisation of copper–dendrimer nanocomposite films

The Cu–dendrimer nanocomposite is suitable for further derivatisation into useful analogues like copper hexacyanoferrate (CuHCF). The cyclic voltammogram exhibits the characteristic features of CuHCF (peak 2) and unreacted copper (peak 1) (Fig. 9).

The morphology of the CuHCF film obtained as above is shown in Fig. 10, which exhibits regular crystalline features with cubical shape. The XRD pattern (Fig. 11) revealed the presence of only a few peaks unlike the randomly oriented crystal features for bulk-formed CuHCF. Only the peaks corresponding to the planes (200), (400) and (311) were observed. The peak corresponding to the (200) plane appears with 100% intensity in the case of bulk-formed, randomly oriented CuHCF, whereas in the present case of the templated CuHCF the intensity of the (200) plane is insignificant. Thus in the presence of the template, the growth is restricted to only a few orientations [40–42]. The appearance high-order planes implies we may end up with crystals with chirality by using this templated approach. Further work in this direction is in progress.

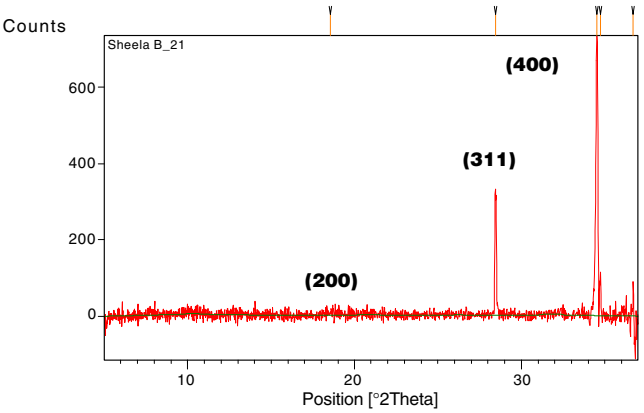

Fig. 11 XRD pattern for copper hexacyanoferrate formed by the electrochemical derivatisation of copper-dendrimer nanocomposite

Conclusions

An electrochemical method for the in situ formation of Cu–dendrimer nanocomposite has been demonstrated for the first time. The loading of copper ions in the dendrimer film can be altered by changing the concentrations of copper ions in the preconcentration solution. This provides a means for preparing dendrimer films with varying concentrations of copper ions and the same can be favourably used for sensing copper ions at ultra trace levels, even in the presence of potentially interfering ions like Bi^{3+} and Cd^{2+} ions. This opens up the possibility of estimating copper ions in biological and environmental samples where trace analysis of copper ions is required. The dendrimers can act as sieves and preconcentrate metal ions, which can be selectively sensed by electrochemical stripping analysis. Furthermore, the copper dendrimer nanocomposite on the electrode can be derivatised electrochemically into stable biomimetic catalytic material like copper hexacyanoferrate.

Acknowledgement The authors wish to thank the funding agencies Defence Research and Development Organisation, New Delhi (DRDO) and Department of Science and Technology, New Delhi (DST) for funding this project. We also acknowledge the Veeco-India Nanotechnology laboratory at JNCASR, Bangalore for the atomic force microscopic images.

References

1. Zeng F, Zimmerman S (1997) Chem Rev 97:1681–1712
2. Bosman AW, Janssen HM, Meijer W (1999) Chem Rev 99:1665–1688
3. Jansen JFGA, de Brabander-van den Berg EMM, Meijer EW (1994) Science 266:1226
4. Jansen JFGA, de Brabander-van den Berg EMM, Meijer EW (1995) J Am Chem Soc 117:4417–4418
5. Zimmerman SC, Wendland MS, Rakow NA, Zharov I, Suslick KS (2002) Nature 418:399–403
6. Archut A, Azzellini GC, Balzani V, De Cola L, Vögtle F (1998) J Am Chem Soc 120:12187–12191
7. Zhao M, Crooks RM (1999) Angew Chem Int Ed 38:364–366
8. Yeung LK, Crooks RM (2001) Nano Lett 1:14–17
9. Scott RWJ, Wilson OM, Crooks RM (2005) J Phys Chem B 109:692
10. Crooks RM, Zhao M, Sun L, Chechik V, Yeung LK (2001) Acc Chem Res 34:81–190
11. Zhao M, Sun L, Crooks RM (1998) J Am Chem Soc 120:4877–4878
12. Niu Y, Yeung LK, Crooks RM (2001) J Am Chem Soc 123:6840–6846
13. Li Y, El-Sayed MA (2001) J Phys Chem B 105:8938–8943
14. Zhao M, Crooks RM (1999) Adv Mater 11:217
15. Ye H, Crooks RM (2005) J Am Chem Soc 127:4930
16. Fonseca ITE, Martin AC, Pletcher D (1987) J Electroanalchem 218:327–329
17. Davis J, Moorcroft MJ, Wilkins SJ, Compton RG (2000) Analyst 12:737–742
18. Tag K, Riedel K, Bauer HJ, Hanke G, Baronian KHR, Kunze G (2007) Sens Actuators B 122:403–409
19. Welch CM, Compton RG (2006) Anal Bioanal Chem 384:601–619
20. Agra-Gutierrez C, Hardcastle JL, Ball JC, Compton RG (1999) Analyst 124:1053–1057
21. Wang H, Huang Y, Tan Z, Hu X (2004) Anal Chim Acta 526:13–17
22. Davis J, Moorcroft MJ, Wilkin SJ, Compton RG, Cardosi MF (2000) Electroanalysis 12:1363–1367
23. Hardcastle JL, Hignette J, Melville JL, Compton RG (2002) Analyst 127:518–524
24. Hardcastle JL, Marcott GG, Compton RG (2000) Electroanalysis 12:559–563
25. Kulesza J, Malik MA, Skorek J, Miecznikowski K, Zamponi S, Berrettoni M, Giorgetti M, Marassi R (1999) J Electrochem Soc 146:3757–3761
26. Zhou DM, Ju HX, Chen HY (1998) J Electroanal Chem 408:219–223
27. Kulesza PJ (1990) Inorg Chem 29:2395
28. Malik MA, Horany G, Kulesza PJ, Inzelt G, Kertesz V, Schmidt R, Czirok E (1998) J Electroanal Chem 452:57–62
29. Neff VD (1985) J Electrochem Soc 132:1382–1387
30. Kaneko M, Okada T (1988) J Electroanal Chem 255:45–52
31. Deng Z, Smyrl WH (1991) J Electrochem Soc 138:1911
32. Kahn O (1995) Nature 378:667
33. Sato O, Einaga Y, Iyoda T, Fujishima A, Hashimoto K (1997) J Phys Chem B101:3903–3905
34. Kulesza PJ, Malik MA, Berrettoni M, Giorgetti M, Zamponi S, Schmidt R, Marassi R (1998) J Phys Chem B102:1870–1876
35. Vergheese TM, Berchmans S (2004) J Electroanalchem 570:35–46
36. Crooks RM, Chechik V, Lemon BL, Sun L, Yeung LK, Zhao M (2002) Synthesis, characterization and applications of dendrimer-encapsulated metal and semiconductor nanoparticles. In: Feldheim DL, Foss CA Jr (eds) Metal nanoparticles, synthesis, characterization and applications. Marcel Dekkar, New York, p 261
37. Lux F, Lemercier G, Andraud C, Schull G, Charra F (2006) Langmuir 22:10874–10876
38. Wuelfing WP, Zamborini FP, Templeton AC, Wen X, Yoon H, Murray RW (2001) Chem Mater 13:87–95
39. Zhang J, Mo Y, Vukmirovic MB, Klie R, Sasaki K, Adzic RR (2004) J Phys Chem B 108:10955–10964
40. Attard GA (2001) J Phys Chem B 105:3158–3167
41. Switzer JA, Kothari HM, Poizot P, Nakanishi S, Bohannan EW (2003) Nature 425:490–493
42. Choudhury S, Bagkar N, Dey GK, Subramanian H, Yakhmi JV (2002) Langmuir 16:7409–7414